THE ASTROPHYSICAL JOURNAL, 473:687–691, 1996 December 20

THE MILKY WAY, LOCAL GALAXIES, AND THE INFRARED TULLY-FISHER RELATION

SANGEETA MALHOTRA,[1,2] DAVID N. SPERGEL,[3,4] JAMES E. RHOADS,[3] AND JING LI[1]
Received 1996 February 27; accepted 1996 July 9

ABSTRACT

Using the near-infrared fluxes of local galaxies derived from *Cosmic Background Explorer* (*COBE*)/Diffuse Infrared Background Experiment (DIRBE)[5] *J*- (1.25 μm) *K*- (2.2 μm), and *L*-band (3.5 μm) maps and published Cepheid distances, we construct Tully-Fisher (TF) diagrams for nearby galaxies. The measured dispersions in these luminosity–line width diagrams are remarkably small: $\sigma_J = 0.09$ mag, $\sigma_K = 0.13$ mag, and $\sigma_L = 0.20$ mag. These dispersions include contributions from the intrinsic TF relation scatter and the errors in estimated galaxy distances, fluxes, inclination angles, extinction corrections, and circular speeds. For the *J* and *K* bands, Monte Carlo simulations give a 95% confidence interval upper limit on the true scatter in the TF diagram of $\sigma_J \leq 0.35$ and $\sigma_K \leq 0.45$.

We determine the Milky Way's luminosity and place it in the TF diagram by fitting a bar plus exponential disk model of the Milky Way to the all-sky DIRBE maps. For "standard" values of its size and circular speed (Sun–Galactic center distance $R_0 = 8.5$ kpc and $\Theta_0 = 220$ km s^{-1}), the Milky Way lies within 1.5 σ of the TF relations.

We can use the TF relation and the Cepheid distances to nearby bright galaxies to constrain R_0 and Θ_0: $1.63 \log (\Theta_0/220 \text{ km s}^{-1}) - \log (R_0/8.5 \text{ kpc}) = 0.08 \pm 0.03$. Alternatively, we can fix the parameters of the Galaxy to their standard values, ignore the Cepheid zero point, and use the TF relation to determine the Hubble constant directly: $H_0 = 72 \pm 12$ km s^{-1} Mpc^{-1}.

We have also tested the TF relation at longer wavelengths, where the emission is dominated by dust. We find no evidence for a TF relation at wavelengths beyond 10 μm. The tight correlation seen in the *L* band suggests that stellar emission dominates over the 3.3 μm polycyclic aromatic hydrocarbon emission.

Subject heading: galaxies: distances and redshifts — galaxies: fundamental parameters — galaxies: photometry

1. INTRODUCTION

The Tully-Fisher (TF) relation between the luminosity and line width of spiral galaxies (Tully & Fisher 1977) has been used extensively as a distance indicator and to map large-scale flows of galaxies (cf. Strauss & Willick 1995 and Jacoby et al. 1992 for reviews). Its usefulness as a distance indicator is limited by the intrinsic scatter of the relation. This scatter is lowest in redder bands where dust extinction is low: *H* band (1.65 μm) (Aaronson, Huchra, & Mould 1979; Aaronson, Mould & Huchra 1980; Aaronson et al. 1986; Freedman 1990; Pierce & Tully 1992) and *I* band (0.90 μm) (Bernstein et al. 1994). In this paper, we extend the TF relation to longer wavelengths. The DIRBE experiment, with its excellent calibration and large beamwidth, is ideal for measuring the total flux of nearby galaxies. The space-based observations also avoid the errors involved in subtracting a large foreground emission at these wavelengths, which becomes problematic for objects with large angular extent. We describe the nearby galaxy data set and present the results of our analysis in § 2.

The Milky Way has often been deemed unsuitable for zero-point calibration of the TF relationship, mainly because of difficulties in estimating its total luminosity. The all-sky DIRBE maps at long wavelengths where dust absorption is small enables the construction of a three-dimensional model for the Milky Way emission. In § 3, we use this model to obtain a measurement of the Galaxy's luminosity. This luminosity can be used to place the Milky Way on the TF diagram with nearby galaxies, to constrain Galactic parameters, and to obtain an independent calibration of the Hubble constant.

2. NEARBY GALAXIES

For this study, we chose a sample of nearby bright spiral galaxies which met the following criteria: (*a*) sizes not too much smaller than the beam, (*b*) measured Cepheid distances, (*c*) no bright stars in a 1° field centered on the galaxy, and (*d*) inclination greater than 45°. We also required that the measured DIRBE flux from the galaxy exceed the week-to-week fluctuations in the DIRBE data. The galaxies used are M31, M33, M81, NGC 300, and NGC 2403. A sixth galaxy, NGC 247, shows a marginal detection and meets our selection criterion in only two bands (*J* and *L*). We will do our analysis both with and without NGC 247. Barring M31 and M33, these galaxies are smaller than the 0°.7 × 0°.7 DIRBE beam. M33 is slightly larger than the beam, and M31 and the Milky Way are extended objects compared with the beam.

The measured fluxes were corrected for extinction using the prescription of Tully & Fouqué (1985), applied to our

[1] IPAC, 100-22, California Institute of Technology, 770 South Wilson, Avenue, Pasadena, CA 91125.
[2] NRC Fellow at NASA Jet Propulsion Laboratory.
[3] Princeton University Observatory, Princeton, NJ 08540.
[4] Department of Astronomy, University of Maryland, College Park, MD 20742.
[5] *COBE* data sets were developed by the NASA Goddard Space Flight Center under the guidance of the *COBE* Science Working Group and were provided by the National Space Science Data Center (NSSDC).

sample using inclination angles from Pierce & Tully (1992) and the standard extinction law from Mathis (1990). These corrections were never large, attaining maximum values of 0.18, 0.07, and 0.03 mag in J, K, and L, respectively, for M31. The distances and distance errors were taken from the published literature as follows: M31 (Freedman 1990), M33 (Freedman, Wilson, & Madore 1991), M81 (Freedman et al. 1994; Hughes et al. 1994), NGC 247 (Catanzarite, Freedman, & Madore 1996), NGC 300 (Freedman 1990), and NGC 2403 (Freedman 1990). Line widths for these galaxies are taken from Pierce & Tully (1992) and Freedman (1990).

2.1. *Flux Extraction*

DIRBE was one of the three experiments on board the *COBE* mission. This experiment observed the entire sky in 10 wave bands (from 1.25 to 240 μm) over a 9 month period. Each point on the sky was observed many times, at a range of solar elongation angles.

This gives a variable viewing geometry from within the interplanetary dust cloud, which is a major source of foreground emission at these wavelengths. A detailed description of the *COBE* mission can be found in Boggess et al. (1992). Details of DIRBE data processing, calibrations, and photometry are given in the DIRBE Explanatory Supplement (Hauser et al. 1995).

The fluxes of the galaxies were derived from the weekly sky maps provided by the DIRBE team. Intensity in each pixel of the weekly map, which is typically half a beam across (and variable across the sky), is a robust average of all observations in a week pointing at the region of the sky in that pixel. Thus, the center of the beam for any observation may be up to half a pixel away from the center of the pixel, and it does not in general lie on the center of the galaxy that lies in that pixel. Since the beam shape is not flat, this can influence the flux measured for that galaxy. This error is estimated to be a few to 9% in the DIRBE Explanatory Supplement (§ 5.6.6). The J-, K-, and L-band fluxes of nearby galaxies derived in this fashion are listed in Table 1.

For each weekly map, we fitted a first-order polynomial to the sky brightness in a small annulus around the pixel that contains the galaxy. The sky background was then subtracted from the maps. A point source can influence the flux levels of neighboring pixels due to the way the weekly maps were made, so pixels adjacent to galaxies were excluded from the sky estimate. All the weekly maps that had observations of that part of the sky were then averaged (after rejecting outliers) to give the average flux of the galaxy. The week-to-week variation of the flux in a given pixel gives an estimate of the noise in the maps. The flux per pixel thus obtained in MJy sr^{-1} is multiplied by the beam size (given in the DIRBE Explanatory Supplement) to derive the flux of the sources.

The flux in a given pixel has contributions from the galaxy, unresolved Galactic stars, and zodiacal light. The zodiacal light varies from week to week as one sees the same part of the sky through a different path length of the zodiacal dust cloud near the Earth. This makes it necessary to remove the background separately for each week. We assume that the starlight is smoothly varying in space and can be subtracted as part of the background. This is true except in the rare case of a very bright star close to the galaxy. We examined the Palomar Observatory Sky Survey plates for such bright stars near candidate galaxies, and we rejected NGC 925 (Silbermann et al. 1996) and NGC 4571 (Pierce et al. 1994) from our sample because of nearby bright stars. Virgo Cluster galaxies are excluded because their proximity to the ecliptic plane makes them hard to detect with the large beam of DIRBE. The week-to-week variation in the flux of the source gives the estimate of errors due to imperfect zodiacal light subtraction, and also due to the beam being centered at different positions with respect to the galaxy. We have used the week-to-week flux variation as a conservative estimate of the errors in the flux measurement.

M33 is slightly bigger than the beam size, and the single pixel method described above underestimates its flux. We simulated observations of M33 assuming an exponential disk with a scale length of 6′ (Regan & Vogel 1994) and the beam profile of the DIRBE beam. In these simulations, we placed the beam randomly within the pixel closest to the position of M33 center. The same experiment was repeated with a point source. The flux measured for the M33 simulation was compared with the flux measured for a point source, and a correction factor of -0.55 mag was added to the M33 magnitude. M31 appears extended in the DIRBE maps, so its flux was measured by summing all the pixels containing the galaxy and normalizing this sum by the ratio of the pixel area to the beam area.

2.2. *Maximum Likelihood Analysis*

We determined the TF parameters and errors using a maximum likelihood analysis. This approach is preferable to a χ^2 fit to the data since the maximum likelihood analysis includes the selection bias due to our magnitude limit (Willick 1994). In a magnitude-limited sample, selection bias implies that galaxies near the luminosity cutoff are systematically brighter (Willick 1994). NGC 247, which falls just below our cutoff, behaves just as expected given this effect: it is brighter than the best-fit TF relation. We perform our analysis both with and without NGC 247.

TABLE 1

DIRBE Measurements of NIR Fluxes of Nearby Galaxies and the Milky Way

Galaxy	Flux in J (Jy)	Flux in K (Jy)	Flux in L (Jy)	μ	log ΔV	A_V
M81	18.8 ± 0.9	16.7 ± 1.0	9.0 ± 0.99	27.8 ± 0.2	2.724	0.36
NGC 300.....	4.6 ± 0.58	3.5 ± 0.7	1.5 ± 0.98	26.5 ± 0.2	2.371	0.14
NGC 2403	5.0 ± 2.00	4.3 ± 1.94	1.6 ± 1.09	27.5 ± 0.3	2.486	0.34
M33	41.2 ± 1.96	35.3 ± 3.15	20.1 ± 0.83	24.5 ± 0.09	2.403	0.32
M31	492.7 ± 49.3	536.2 ± 53.6	281 ± 28.1	24.4 ± 0.1	2.737	0.93
NGC 247.....	1.7 ± 1.06	0.8 ± 1.5	0.62 ± 0.86	27.9 ± 0.2	2.362	0.46
Milky Way.....	$(2.6 \pm 0.26) \times 10^{12}$	$(2.35 \pm 0.23) \times 10^{12}$	$(1.22 \pm 0.12) \times 10^{12}$	0 ± 0.23	2.68	0.00

The maximum likelihood function for our sample is

$$P(\boldsymbol{m} \mid a, b, \sigma_{\rm TF}) = \prod \frac{\exp - [m_i - D_i - (a\eta_i + b)]^2/2\sigma_{\rm TF}^2}{\int_{-\infty}^{m_{l,i}} \exp [m' - D_i - (a\eta_i + b)]^2/2\sigma_{\rm TF}^2 \, dm'} . \quad (1)$$

Here the observed quantities are the galaxies' magnitudes m_i, Cepheid-based distance moduli D_i, the logarithms of their line widths η_i, and the magnitude limits $m_{l,\,i}$ (i.e., the amplitude of the week-to-week fluctuations measured at the galaxy location). The model parameters a, b, and $\sigma_{\rm TF}$ are the slope, zero point, and (total) scatter about the TF relation, respectively. Note that $\sigma_{\rm TF}$ includes contributions from both the intrinsic TF relation scatter and the errors in estimated galaxy distances, fluxes, inclination angles, extinction corrections, and circular speeds. The product is evaluated over all galaxies in the sample, i.e., all galaxies for which $m_i < m_{l,i}$.

The maximum likelihood fits to the J-, K-, and L-band TF relations (Figs. 1, 2, and 3) are

$$J^c = -8.13^{+0.41}_{-0.42} \log (\Delta V/400 \text{ km s}^{-1}) - 22.00^{+0.12}_{-0.12} ,$$

$$K^c = -8.59^{+0.67}_{-0.65} \log (\Delta V/400 \text{ km s}^{-1}) - 23.01^{+0.11}_{-0.11} ,$$

$$L^c = -9.01^{+0.96}_{-0.94} \log (\Delta V/400 \text{ km s}^{-1}) - 22.99^{+0.14}_{-0.17} ,$$

where J^c, K^c, and L^c are extinction-corrected magnitudes. The line width–luminosity, or TF, relation in these bands is very tight, showing a scatter of $\sigma_{\rm TF}(J) = 0.09$ mag in the J band, $\sigma_{\rm TF}(K) = 0.13$ mag in the K band, and $\sigma_{\rm TF}(L) = 0.20$ mag in the L band. The χ^2 fits yield smaller (but less believable) values for σ. The minimization of the likelihood function was done with the Numerical Recipes' (Press et al. 1993) AMOEBA program. Investigation of the likelihood surface showed that it was well behaved near its minimum. A small scatter in the TF relation of five galaxies implies a small intrinsic scatter in the TF relation for all galaxies. We confirm this for our sample with a Monte Carlo simulation with 1000 realizations of the local galaxies sample. We generated five galaxies with the reported η_i and our best-fit slopes. We varied the value of $\sigma_{\rm TF}$ in our simulations. For a true $\sigma_{\rm TF}(J) = 0.35$, we recovered a scatter as small as

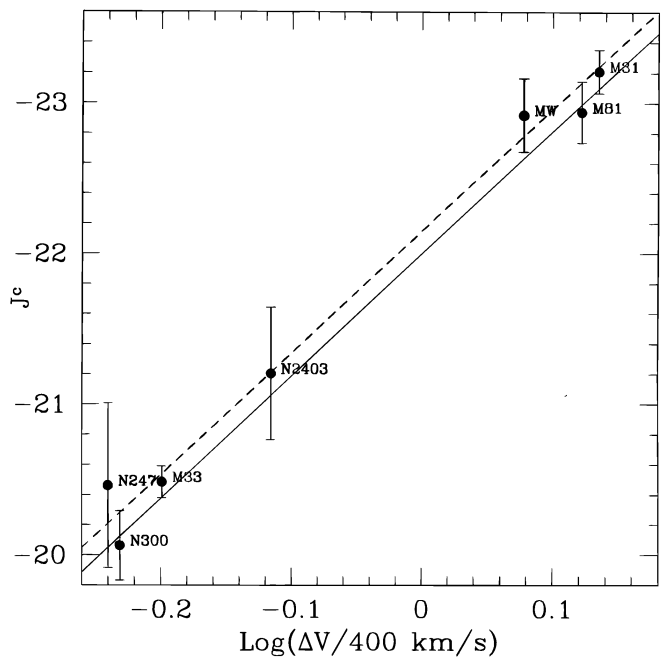

FIG. 1.—The J-band (1.25 μm) TF diagram. The error bars for the local galaxies M31, M81, NGC 2403, M33, NGC 300, and NGC 247 represent the 1 σ uncertainties in the extinction-corrected absolute J-band magnitude (J^c) due to photometric errors and reported uncertainties in Cepheid distances, added in quadrature. The MW absolute magnitude assumes a Galactocenteric distance of 8.5 ± 0.5 kpc and circular speed $\Theta_0 = 220 \pm 10$ km s^{-1}; its error bar represents the 0.23 mag uncertainty derived in § 3. The solid line is the fit to the five-galaxy sample, excluding NGC 247 (which falls just below our magnitude limit) and the Milky Way. The dashed line is the fit to the full seven-galaxy sample.

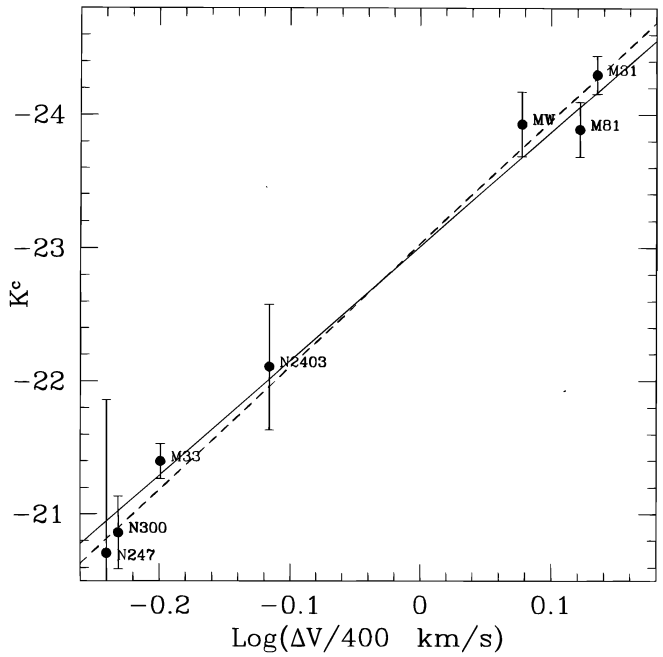

FIG. 2.—Same as in Fig. 1, but for the K band (2.2 μm)

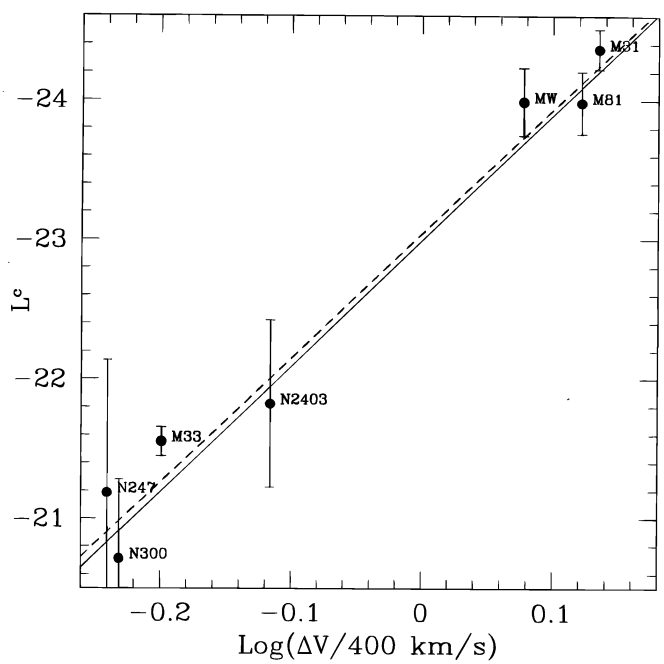

FIG. 3.—Same as in Fig. 1, but for the L band (3.5 μm)

observed in less than 5% of the simulations. For $\sigma_{TF}(J) = 0.55$, we recovered such a small scatter in only 1% of the simulations. The quoted errors on the TF slope and zero point are the 95% confidence intervals from the Monte Carlo simulations.

If we include NGC 247 in the sample, then the maximum likelihood fits are

$$J^c = -7.78 \log (\Delta V/400 \text{ km s}^{-1}) - 22.07 ,$$

$$K^c = -8.90 \log (\Delta V/400 \text{ km s}^{-1}) - 22.99 ,$$

$$L^c = -8.76 \log (\Delta V/400 \text{ km s}^{-1}) - 23.00 ,$$

and the corresponding TF relation scatter is $\sigma_J = 0.15$, $\sigma_K = 0.14$, and $\sigma_L = 0.21$ mag. For a true $\sigma_{TF}(K) = 0.45$, we found such small scatter in less than 5% of simulations. For $\sigma_{TF}(K) = 0.7$, we found such smaller scatter in only 1% of simulations.

The dust emission at longer wavelengths 60–240 μm does not show a luminosity–line width relation. From this and from the tight L-band TF correlation, we conclude that the nonstellar or dust contribution to the L band is not large. This is consistent with recent estimates of 8%–16% contribution of the 3.3 μm polycyclic aromatic hydrocarbon feature to the L band (Bernard et al. 1994).

While giant stars are thought to contribute most of the light in near-IR bands, supergiants can make an important contribution in the spiral arms (Rhoads 1996). This contribution does not appear to be a source of significant scatter in the TF relation.

3. THE MILKY WAY

We cannot directly use the total flux from the Milky Way (MW) because regions at different distances contribute to that flux. We estimated the luminosity density of the MW from the best-fitting model to the DIRBE data. The MW was modeled as a sum of an exponential disk and a bar (Spergel, Malhotra, & Blitz 1996, hereafter Paper I). Extinction corrections were based on a three-dimensional dust model. Varying modeling parameters and extinctions changes the MW flux by less than 10%, and thus we assume a 10% modeling error (Paper I). For Galactic parameters, we assume a circular speed $\Theta_0 = 220 \pm 10$ km s^{-1} and a distance to the Galactic center $R_0 = 8.5 \pm 0.5$ kpc (Gunn, Knapp, & Tremaine 1979). Using these values, we obtain absolute magnitudes $J = -23.05$, $K = -24.06$, and $L = -23.88$. More recent determinations of the Sun–Galactic center distance using water masers suggest a smaller distance: 7.1 ± 1.5 kpc (Reid et al. 1988) and 8.1 ± 1.1 kpc (Gwinn, Moran, & Reid 1992). Combining our uncertainties and assuming a TF slope of 9 implies an intrinsic uncertainty in the Galaxy's position in the TF diagram of 0.23 mag.

If we include the Milky Way in the sample, then the maximum likelihood fits are

$$J^c = -8.09 \log (\Delta V/400 \text{ km s}^{-1}) - 22.15 ,$$

$$K^c = -9.23 \log (\Delta V/400 \text{ km s}^{-1}) - 23.03 ,$$

$$L^c = -8.91 \log (\Delta V/400 \text{ km s}^{-1}) - 23.04 .$$

For uniformity, the velocity width of the MW was scaled from the observed velocity width of M31: $\Delta V(\text{MW}) = (220/250)\Delta V(\text{M31})$. The TF relation in these bands remains very tight with $\sigma_J = 0.18$, $\sigma_K = 0.16$, and $\sigma_L = 0.21$. We repeated the Monte Carlo simulations as described in § 2. For a true $\sigma_{TF}(K) = 0.45$, we found a scatter as small as observed in less than 5% of the simulations. For $\sigma_{TF}(K) = 0.57$, we found such a small scatter in only 1% of the simulations. With the standard parameters, the Milky Way is $\sim 1.5\ \sigma$ too luminous in J, $\sim 1\ \sigma$ too luminous in K, and $\sim 1.4\ \sigma$ too luminous in L. This basic agreement shows that the Cepheid distance scale is consistent at the 10% level with the Gunn et al. (1979) distance determination to the Galactic center.

Alternatively, we can use the TF relation obtained for the five-galaxy sample, together with our model for the Galactic luminosity, to constrain Galactic parameters:

$$-5 \log \left(\frac{R_0}{8.5 \text{ kpc}} \right) + 8.13 \log \left(\frac{\Theta_0}{220 \text{ km s}^{-1}} \right) = 0.42 \pm 0.16 ,$$

$$-5 \log \left(\frac{R_0}{8.5 \text{ kpc}} \right) + 8.59 \log \left(\frac{\Theta_0}{220 \text{ km s}^{-1}} \right) = 0.39 \pm 0.19 ,$$

$$-5 \log \left(\frac{R_0}{8.5 \text{ kpc}} \right) + 9.01 \log \left(\frac{\Theta_0}{220 \text{ km s}^{-1}} \right) = 0.43 \pm 0.24 ,$$

where the three equations correspond to fitting the J-, K-, and L-band relations, respectively. The uncertainties include the width of the TF relation, the quoted uncertainties in the Galactic model (10%), and a conservative estimate of systematic errors in point-source flux measurements (9%). This comparison of the Galaxy with the sample of nearby galaxies suggests that its rotation speed is unlikely to be as small as 200 km s^{-1}.

We can also use the Galaxy (if we are willing to assume values for R_0 and Θ_0) to obtain an absolute calibration that is independent of the zero point of the Cepheid distance scale (Wright 1994). To go from this zero point to a measurement of the Hubble parameter, we need flux and line width data for more distant galaxies whose recessional velocities are dominated by Hubble flow. Such data are most readily available for the 1.6 μm H band (Aaronson et al. 1986). We have therefore combined our J- and K-band photometry with published $H_{-0.5}$ magnitudes (Freedman 1990; Pierce & Tully 1992) in order to determine the extinction-corrected $H^c_{-0.5} - K^c$ and $J^c - K^c$ color-color relation for the galaxies in this local galaxies sample. A χ^2 fit to the data yields $(H^c_{-0.5} - K^c) = 3.27 - 2.50(J^c - K^c)$ with a scatter of 0.18 mag. This suggests $(H^c_{-0.5} - K^c) = 0.75 \pm 0.18$ and hence $H^c_{-0.5} = -23.31$ for the Milky Way.

We can use this estimate to set a zero point for the H-band TF relation. Combining this zero point with the slope of the H-band TF relation from the Coma Cluster (data in Table 2 of Aaronson et al. 1986) then yields a distance to Coma and a measurement of the Hubble constant, independent of the distance ladder. From 13 Coma galaxies, we derive a slope of the H-band TF relation to be 9.26, which is consistent with the slope derived for local galaxies in the K band in this section. Using this slope and the zero point from the Milky Way luminosity, we derive a Hubble constant $H_0 = 72 \pm 12$ km s^{-1} Mpc^{-1}. The error bar is derived by adding in quadrature the uncertainty in the MW luminosity and the spread in the Coma Cluster TF relation. Since the MW lies in the middle of the range in velocity width (ΔV), slightly different slopes of the TF relation should not affect the mean distance to the Coma Cluster too much. The dependence of H_0 on Galactic size

and rotational velocity is more substantial, and is given by

$$H_0 = 72 \text{ km s}^{-1} \text{ Mpc}^{-1}(8.5 \text{ kpc}/R_0)(\Theta_0/220)^{1.852} .$$

If we assume that $R_0 = 7.1$ kpc (the smaller maser-based measurement [Reid et al. 1988]) and hold Θ_0 constant, then the Hubble constant estimate increases to 86 km s^{-1} Mpc^{-1}. If we assume that $R_0 = 7.1$ kpc and hold the angular rotation rate Θ_0/R_0 constant, then the Hubble constant estimate decreases to 62 km s^{-1} Mpc^{-1}. Besides the uncertainty in Galactic parameters, the dominant source of error in these estimates is the extrapolation from J- and K-band fluxes to the H band. Thus, a K-band survey of spirals in the Coma Cluster would yield a more definitive value of the Hubble constant.

4. CONCLUSIONS

We find that the TF relation extends to longer wavelengths (2.2 and 3.5 μm) than previously explored. The extinction corrections (cf. Mathis 1990) at 2.2 and 3.5 μm are about half and one-third as large as for the H band at 1.65 μm, so these bands may be usefully exploited for distance estimation. The scatter in the TF relation for these bands is small, comparable to or smaller than the small scatter found for I and H bands (Freedman 1990; Pierce & Tully 1992; Bernstein et al. 1994). With the advent of imaging IR instruments and two major near-IR sky surveys (2MASS and DENIS), there is also the potential to estimate the distances, and hence the peculiar velocity flows, for many more galaxies ($\sim 10^6$) in a greater part of the sky and nearer to the plane of the Milky Way.

Using Cepheid distances for galaxies in the Local Group (not including the Milky Way) and assuming standard Galactic parameters, we find that the Galaxy obeys the TF relation for nearby galaxies with Cepheid distances. This consistency is an independent check of the Cepheid distances and of Galactic parameters.

We thank Leo Blitz, George Helou, Jill Knapp, Barry Madore, Nancy Silbermann, and Ned Wright for discussions and suggestions, and David Leisawitz for answering questions about the DIRBE data. We also thank Michael Strauss for helpful comments on an earlier version of this manuscript, and the referee for thorough refereeing. This work made use of NASA Extragalactic Database NED. This work was partially supported by NASA ADP NAG5-269.

REFERENCES

Aaronson, M., Huchra, J., & Mould, J. 1979, ApJ, 229, 1
Aaronson, M., Mould, J., & Huchra, J. 1980, ApJ, 237, 655
Aaronson, M., Bothun, G., Mould, J., Huchra, J., Schommer, R. A., & Cornell, M. E. 1986, ApJ, 302, 536
Bernard, J. P., Boulanger, F., Désert, F. X., Giard, M., Helou, G., & Puget, J. L. 1994, A&A, 291, L5
Bernstein, G. M., Guhathakurta, P., Raychaudhary, S., Giovanelli, R., Haynes, M. P., Herter, T., & Vogt, N. 1994, AJ, 107, 1962
Boggess, N. W., et al. 1992, ApJ 397, 420
Catanzarite, J. H., Freedman, W. L., & Madore, B. F. 1996, in preparation
Freedman, W. L. 1990, 355, L35
Freedman, W. L., Wilson, C. D., & Madore, B. 1991, ApJ, 372, 455
Freedman, W. L., et al. 1994, ApJ, 427, 628
Gwinn, C. R., Moran, J. M., & Reid, M. J. 1992, ApJ, 393, 149
Gunn, J. E., Knapp, G. R., & Tremaine, S. 1979, AJ, 84, 1181
Hauser, M. G., Kelsall, T., Leisawitz, D., & Weiland, J. 1995, The DIRBE Explanatory Supplement (http://www.gsfc.nasa.gov/astro/cobe/dirbe_exsup.html)
Hughes, S. M. G., et al. 1994, ApJ, 428, 143
Jacoby, G., et al. 1992, PASP, 104, 599
Mathis, J. S. 1990, ARA&A, 28, 37
Pierce, M. J., & Tully, R. B. 1992, ApJ, 387, 47
Pierce, M. J., Welch, D. L., McClure, R. D., van den Bergh, S., Racine, R., & Stetson, P. B. 1994, Nature, 371, 385
Press, W. H., Teukolsky, S. A., Vetterling, W. T., & Flannery, B. P. 1993, Numerical Recipes (New York: Cambridge Univ. Press)
Regan, M., & Vogel, S. 1994, ApJ, 434, 536
Reid, M. J., Schneps, M. H., Moran, J. M., Gwinn, C. R., Genzel, R., Downes, D., & Rönnäng, B. 1988, ApJ, 330, 809
Rhoads, J. E. 1996, ApJ, submitted
Silbermann, N. A., et al. 1996, ApJ, 470, 1
Spergel, D. N., Malhotra, S., & Blitz, L. 1996, in preparation (Paper I)
Strauss, M. A., & Willick, J. A. 1995, Phys. Rep., 261, 271
Tully, J. B., & Fisher, J. R. 1977, A&A, 54, 661
Tully, J. B., & Fouqué, P. 1985, ApJS, 58, 67
Willick, J. A. 1994, ApJS, 92, 1
Wright, E. 1994, BAAS, 185, 32.05